I&EC research
Industrial & Engineering Chemistry Research

Review

pubs.acs.org/IECR

A Review: Synthesis of Carbon-Based Nano and Micro Materials by High Temperature and High Pressure

Alireza Bazargan, Ying Yan, Chi Wai Hui, and Gordon McKay*

Department of Chemical and Biomolecular Engineering, Hong Kong University of Technology, Clearwater Bay, Hong Kong

Supporting Information

ABSTRACT: This review covers the production of solid carbonaceous materials at high temperatures (above 500 °C) and high pressures. The review orders the high temperature/high pressure (HTHP) studies by their final product categories, namely carbon spheres, prolate spheroids (also known as ellipsoids and olivaries), nanotubes, and others such as diamonds, fullerenes, composites, and nanostars. The mechanisms as well as the properties of the products are discussed. In particular, the literature pertaining to the production of carbon ellipsoids has been collected for the first time. On one hand, the review concludes that, due to the existence of other conventional and more practical methods, the production of nanotubes and spheres via HTHP does not appear to be industrially feasible. On the other hand, using the HTHP method to produce olivary carbons and other new and exotic products seems attractive due to the absence of conventional methods for their production.

1. INTRODUCTION

Carbon is one of the most versatile elements in the Mendeleev table of elements. In previous decades, much research has been conducted on producing various carbon products, and today carbon-based materials have wide-ranging applications. Numerous researchers have worked on developing innovative carbon-based products including carbon nanotubes, nanorods, spheroids, spherules, glassy carbons, onions, fullerenes, and carbon composites among various others.[1,2]

Among the research pertaining to the production of useful materials through the thermal decomposition of carbonaceous feeds, there has been a wide array of scrutinized parameters which affect the final product. These parameters include—but are not limited to—the heating rate, the holding time, the structure of the reactor, the use of catalysts, the use of solvents, and the pressure of the system.

The subject of carbonization under pressure is more than a century old. As an example, J. B. Hannay attempted to produce diamonds by heating a mixture of hydrocarbons, bone oil, and lithium at red heat in sealed wrought-iron tubes in 1880. The experimental conditions were so extreme that only three of the eight iron tubes survived without explosion.[3] An example of carbonization in the 1950s is the gastight thermolysis of anthracene at 600 °C.[4] The topic of mesophase pitch carbonization has also been under wide examination for decades.[5−16] Much of the research in the area is concerned with coal and/or coke.[17−27] Other studies also exist which do not closely consider the solid products of pressurized thermolysis, but rather the gases.[28−31] The subject area of carbonization under pressure is not new. Nonetheless, there are still many gaps in the field, new discoveries are made, and a lot of work remains to be done.

Inagaki and co-workers have provided a review of carbonization under pressure.[32] Therein, a limited number of articles regarding the decomposition behavior and resulting products at pressures higher than atmospheric are reviewed. Inagaki has been one of the influential researchers in this regard, publishing articles on the subject from as early as 30 years ago.[33−39] More recently Chemii has written a very short review which includes some articles regarding pressurized carbonization of systems containing carbon dioxide. Unfortunately, the review is in the Polish language and hence is not easily understood by the majority of readers.[40] Pol and co-workers have also provided a review on the subject but have only focused on the numerous papers regarding their own method of carbonization under pressure, i.e. a dry autoclaving process without the use of a solvent or catalyst.[41] Thus, the previously published reviews on the thermal treatment of carbonaceous feeds under pressure are discrete, far from exhaustive, and exclude many relevant references.

In order to better organize the literature in this regard, the current review paper has been prepared so that only the publications pertaining to the simultaneous existence of high pressure and high temperature (higher than 500 °C) are considered. This is a crucial identifier because countless studies exist which consider only one of the two parameters: i.e. studies which consider carbonization under high temperatures (but not high pressures),[42−44] and those which consider carbonization under high pressures (but not high temperatures).[45−50] However, studies which consider the carbonization of precursors under both high temperatures and high pressures are more scarce. The reason for setting 500 °C as the cutoff temperature for the review is that the highest temperature at which traditional pressurized stainless steel reactors operate is 500 °C. Above this operating temperature, pressurized systems require specialized alloys and expensive equipment, and hence, the existing literature is a lot less frequent. It should also be noted that the term "high pressure" must be understood in a relative manner. In fact, the pressures discussed herein would

Received: June 11, 2013
Revised: August 5, 2013
Accepted: August 5, 2013
Published: August 5, 2013

dx.doi.org/10.1021/ie4018513 | Ind. Eng. Chem. Res. 2013, 52, 12689−12702

be considered moderate or even low when compared to the extreme processes at pressures above 1 GPa and the "diamond stable" region.[51] Selected examples of studies which did not fit the scope[52] defined for the review can be seen in Table S1 of the Supporting Information.

2. VARIOUS CARBON PRODUCTS FROM HIGH TEMPERATURE/HIGH PRESSURE CARBONIZATION

There are a variety of carbonaceous products which can be produced from a pressurized thermal degradation system. Herein, the studies are ordered on the basis of the final as-prepared product and are divided into the general categories of carbon spheres, prolate spheroids, nanotubes, and others.

2.1. Spheres. One of the most common particles seen in high temperature/high pressure (HTHP) systems are carbon spheres. In the late 1970s and beyond, Inagaki et al.[33−39] pyrolyzed polymeric materials such as polyethylene (PE), polyvinylchloride (PVC), polypropylene (PP), polyvinylidene chlorine (PVDC), and others inside a sealed gold tube under gas pressures of 10−30 MPa. The researchers sealed PE in thin-walled collapsible gold tubes so that by collapsing the tube, the volume of the gas inside could be reduced. The tube was placed in a Stellite bomb, and the temperature was then increased by the use of an external furnace to 300−650 °C at a rate of 3 °C/min. The nitrogen gas within the bomb was controlled and leaked throughout the experiment so that isobaric conditions could be maintained. Under 30 MPa no carbonization was seen up to 500 °C, and white solids were found. An abrupt pressure increase was observed at about 530 °C, and as the temperature was raised between 540 and 600 °C, viscous pitchlike material was formed. This material contained a large volatile fraction discerned by the fact that, after the experiment had finished, it lost weight with time in air. If a specialized autoclave was used instead of the gold tubes, the yields fell to about 30% from about 43%. The volatile matter within the solid product was examined with liquid chromatography and was found to consist of parafins, olefins, and aromatics with a small number of rings. The increase of the residence time within the reactor resulted in an increase of solid yield. When only 10 MPa of pressure was exerted, the temperatures at which the phenomena were observed shifted to lower amounts by about 40 °C. Five MPa of pressure proved to be inadequate, as the pressure increase inside the gold tube due to polymer decomposition surpassed the external pressure and resulted in the rupture of the tube. Different types of carbon products were seen, including carbon spheres and flakes. The addition of even small amounts of PVC favored the production of carbon spheres and hindered the production of flakes. If larger amounts of PVC were added, the spheres tended to link together. More than 70% PVC completely eliminated the production of separate spheres. Results indicated that PVC and PE decomposed independently. However, after their independent decomposition and formation of pitchlike liquid, they cocarbonized. In order to see if chlorine in the gas phase had an effect on sphere formation, the emerging gas during decomposition was replaced with argon before the samples were carbonized under pressure. It was seen that the presence of chlorine gas is not necessary for sphere production. The polymerization degree of the precursors did not affect the product either. If PVDC was added, the size of the spheres decreased, while the addition of PP made them bigger. Polystyrene (PS) hindered sphere production. Generally the size of the spherules produced from PE ranged from 1 to 3 μm. At 600 °C aggregated particles coexisted with spheres, but at 650 °C the aggregated particles faded away, and only separate spheres were seen. It should be noted that, although the pressures in the studies of Inagaki et al. were high, they were lower than the 125 MPa exerted by Hiarno, Naka, et al. for the production of carbon spheres from divinylbenzene.[53]

The researchers postulated that the flaky carbon which deposited on the walls of the tube came from the gas phase, while the spherules found at the bottom were formed by liquid-phase carbonization. Longer residence times did not change the yield but helped to separate the spheres. If the residence time was extended to 20 h, connections between spherules seemed to reemerge, and a slight decrease in yields was seen. The researchers concluded that two general conditions exist for sphere production from polymers: (1) the formation of active carbon chains and (2) the formation of intermediary low-molecular weight residues.

Upon examining the nanotexture of the spheres, it was concluded that aromatic layer planes have aligned preferentially on circular conical surfaces. As can be seen in Figure 1, these

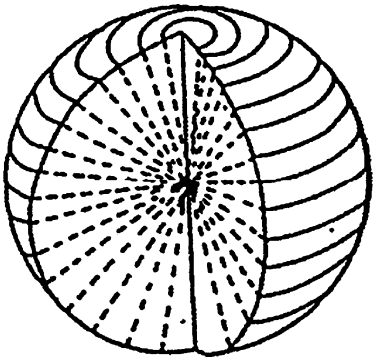

Figure 1. Nanotexture of the HTHP spheres.[32]

cones which have a common vertex in the center of the sphere have an axis of symmetry connecting the two poles of the sphere. Extreme heat treatment of the spheres at 3000 °C somewhat deformed them into flattened spherules and thick disks, forming cracks along the aromatic layers. The graphitizability of the carbon spheres was low. This may have been due to the size effect of their primary particles. The nongraphitizing carbons were composed of small spherical shells with a mean size of 7−10 nm. These shells were not independent of their neighbors and restrained one another, thus hindering crystallite growth.[38]

Inagaki et al. went on to assess the pressure pyrolysis of various precursors for microsphere production. Trends regarding the carbon atom ratios of the precursors for sphere production were observed.[39] Some years later Inagaki was involved in the authorship of a pair of articles which extensively addressed the mechanism of carbonization under pressure including the influence of aromaticity and impurities.[54,55]

More recently Q. Chen's research group has published numerous papers on pyrolysis under pressure, usually in the presence of alkali metals as catalysts. In one study which used metallic lithium as the reducing agent alongside carbon dioxide in a closed stainless steel system, at 280 °C no solid products were seen.[56] With the increase of temperature to 550 °C carbon nanotubes become the major product. The researchers observed that at a temperature of 650 °C (held for 10 h at 1000 atm) supercritical carbon dioxide molecules were absorbed and reduced by liquid Li, while the nanodroplets of

the metal also acted as templates for growth of spheres. Nanospheres with diameters predominantly in the range of 360−600 nm accounted for about 30% of the solid product, while carbon nanotubes, graphite, and amorphous carbon composed the rest. The surface of the spheres crystallized due to the high temperatures, but as the outer graphical shells develop, the crystallization process did not continue inward. This was because the graphical layers inhibited thermal conduction to the interior layers which therefore remained amorphous. Most of the nanospheres were full, while some hollow spheres were also found.

Metallic calcium has also been used for reducing supercritical carbon dioxide for the production of smooth 1−2 μm carbon spheres. Temperatures lower than 450 °C did not initiate the reaction, while at 500 °C the products were predominantly nanorods and graphite. At 550−600 °C and beyond, carbon spheres became the major products (80%) with larger sizes and more defects and disorders. The mechanism was thought to be as follows: first, the metallic Ca atom bonds with the oxygen present in the carbon dioxide to form CaO and CO. Then the calcium reacts with CO to form nanogranular carbon. The possibility of the decomposition of CO to form CO_2 and C is not entirely ruled out. However, it is less prevalent due to the presence of excess amounts of carbon dioxide. At high temperatures the nanogranules will move fiercely and roll on the surface of the metallic calcium, incorporating new carbon atoms to form perfectly round spheres due to the statistical rule of thermal movement.[57]

Polyethylene terephthalate (PET) along with carbon dioxide has also been used under autogenic pressures at 500−700 °C for 3 h for carbon sphere production.[58] This method is particularly attractive because the precursor can be waste plastic. With the increase of temperature the PET breaks down into aromatic hydrocarbons (such as benzene, toluene, biphenyl, etc.), and small gaseous molecules such as CO_2 and H_2O. In the temperature range of 400−500 °C the aromatic molecules in turn dissolve in the supercritical carbon dioxide to form a homogeneous mixture. As temperatures increase and time passes, clusters begin to condense and produce highly aromatic carbon microspheres 1−5 μm in diameter. A two-dimensional disorder exists in the basal plane. Although prolonged heating times at 650 °C do not affect the size significantly, higher temperatures result in higher graphitization, a narrow size distribution, a higher yield, and more spherical products. At lower temperatures and with lower holding times, polynuclear aromatic hydrocarbons with a low degree of alkyl substitution and aromatic condensation or conjugation are seen. Altering the size of the initial PET feed affects the morphology of the product. If less amounts of carbon dioxide are used, more amorphous carbon and irregular particles appear.

Various hydrocarbons with 5−14 carbon atoms in their chain such as pentane, cyclohexane, camphorquinone, xylene, mesitylene, camphene, decahydronaphthalene, diphenylmethane, and anthracene were treated in a closed autoclave held at 700 °C for 3 h (Figure 2).[59] It was theorized that clusters composed of aromatic rings and aliphatic chains will form in the midst of the supercritical fluid conditions within the autoclave. In order to minimize the interfacial energy inside the highly reducing atmosphere, these clusters will arrange themselves so that the aliphatic tails are exposed to the fluid, while the rings remain separated from the fluid inside the colloid similar to a core. These cores in turn solidify and form

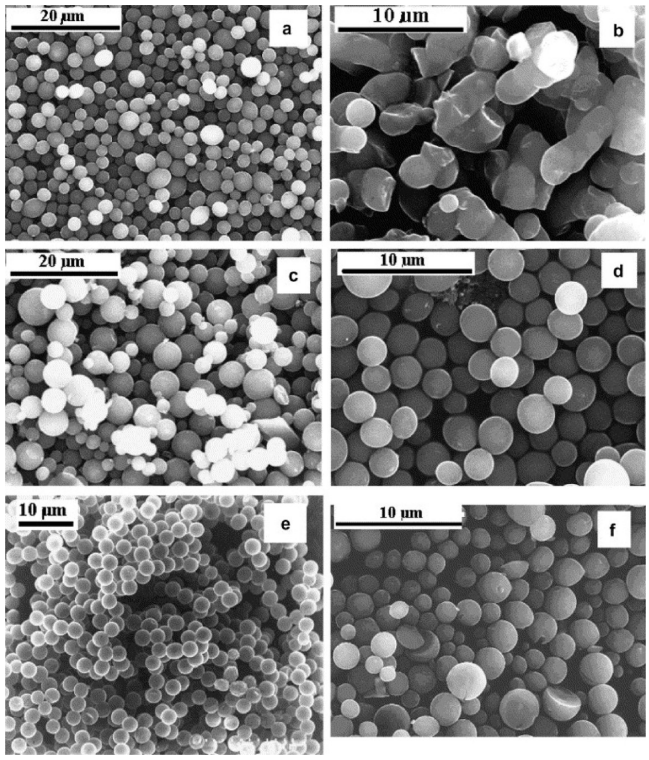

Figure 2. Scanning electron micrographs of (a) pentane, (b) cyclohexane, (c) camphorquinone, (d) xylene, (e) mesitylene, and (f) camphene treated in a closed cell at 700 °C for 3 h.[59]

carbon spheres. The faster the nucleation is, the more numerous the small carbon spheres may be. Since the spheres are nonagglomerated as opposed to a monolithic product, the researchers postulated that a gas-to-particle or gas-to-droplet conversion has taken place. The spheres were more than 99% carbon, and further heat treatment under an inert atmosphere at 950 °C increased the purity to above 99.9%. Along with the spheres, flakes and carbon sheets were also obtained. Evidently the C:H ratio plays an important role in flake production. So long as the C:H ratio of the initial feedstock is lower than 1:1 (for example 5:12 for pentane) enough hydrogen will exist in the system which caps the edge sites during carbonization. If enough hydrogen is not present, polymerization takes place, fluidity is decreased, and flakes are formed instead of spheres. The solid yield is about 90% of the maximum theoretical yield. The remaining 10% of the carbon is thought to form light C_xH_y gases as seen in previous experiments. The researchers went on to compare their results with those of Kroto et al. who used a continuous CVD system for carbon sphere production in which longer feed times formed larger particles.[60] These results seem to concur with the static closed autoclave, because such a system can be equated with a CVD unit having a very long feeding time which leads to larger spherical products.[59]

In a hydrothermal study for producing spheres, water was used as a solvent and soluble starch as the carbon source.[61] At lower temperatures the starch broke down to glucose and levulose due to hydrolysis. Further dehydration took place, and colloidal carbon nanospheres with uniform size were formed due to polymerization (see Figure 3). As the temperature increased to 300−400 °C, the colloids moved at an accelerated pace and self-assembled to form spherical aggregates. As the temperature increased even further to 600 °C, the number of functional groups in the colloidal carbon spheres decreased and

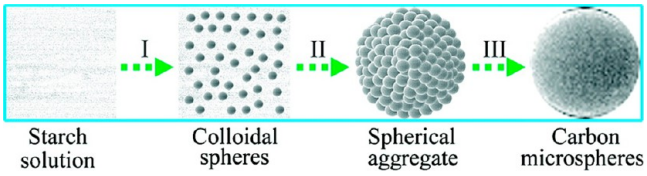

Figure 3. Formation of carbon microspheres from the aggregation of smaller spherical colloids. [printed with permission from Zheng, M.; Liu, Y.; Xiao, Y.; Zhu, Y.; Guan, Q.; Yuan, D. An Easy Catalyst-Free Hydrothermal Method to Prepare Monodisperse Carbon Microspheres on a Large Scale. *J. Phys. Chem. C* **2009**, *113*(19), 8455–8459.][61]

the colloids fused to form solid carbon microspheres. The resulting product was soft, light, cottonlike, smooth, and functionalized with hydroxyl and carboxyl groups with a yield of about 95% (considering the 40% carbon weight percent of starch). Almost 100% of the solid product was in the form of monodispersed carbon microspheres with a diameter of about 1.8–2 μm. Trace amounts of nanospheres were also found. It was postulated that these spheres could be used in biochemistry, drug delivery, as catalyst supports, and as templates for fabricating other structures. The size of the final product could be controlled as it was found to be a function of the concentration of the feed as well as the reaction temperatures. As the initial concentration is increased, the size of the spheres increases, while their dispersibility diminishes. If other variables are kept constant, the size of the resulting spheres is less under lower temperatures. Strangely, if temperatures decrease to as low as 450 °C, an abnormal increase in size and diameter distribution is witnessed. In addition, the high heating rate of 10 °C min^{-1} plays a key role in the small size and narrow size distribution. Under lower heating rates, larger carbon spheres are obtained with a wide size distribution.

In one of the earliest works of Pol, Gedanken, and coworkers, mesitylene is used as a carbon source in an autoclave which is heated up to 700 °C at 5 °C per minute and held for 3 h.[62] Surprisingly although the article claims to have discovered a "novel" method, this is not entirely accurate as similar dry autoclaving methods had been used decades earlier.[4] Instead of using an expensive reactor, the researchers used a stainless steel reaction cell comprising a standard union piece capped off at both ends. Figure 4 shows the cell which the researchers also refer to as an "autoclave". Nongraphitic, perfectly spherical,

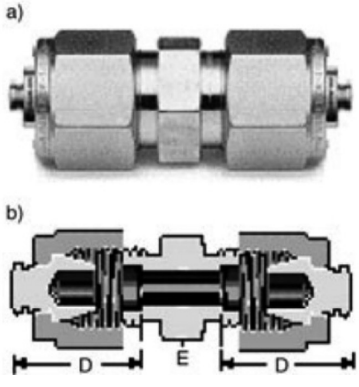

Figure 4. (a) Overview of the union piece used and (b) cross section of the system showing the caps and union; D: cap, E: union.[63]

monodispersed carbon spheres are produced (2.5 ± 0.05 μm). It is concluded that, although the solid spheres are smooth and hard, they do have minor hills and valleys that slightly increase the surface area compared to the calculated surface of a perfectly smooth spherule with the same diameter. The researchers also noticed that, if the vessel is quickly cooled from 700 °C rather than set to cool naturally in the ambient environment, sausagelike structures are formed instead of spheres. The size of the spheres is not dependent on the reaction temperature, the amount of the precursor, the surrounding inert gas type, or the heating holding time. Interestingly, it was also concluded that the change of enthalpy from the mesitylene precursor to the 2.5 μm spherical product is close to zero.

In another experiment, Pol et al. tried using a silicon source (TEOS) within their setup.[64] The temperature of the closed autogenic system was raised to 700 °C at 5 °C min^{-1} and held for one hour. Monodisperesed carbon spheres were once again obtained, but this time covered with silicon. The carbon cores had a diameter range of 0.3–1 μm, while the silicon nanocoating had a thickness of 8–15 nm. The product yield was approximately 38%.

Various types of waste plastics (low density polyethylene (LDPE), high density polyethylene (HDPE), polyethylene terephthalate (PET), polystyrene (PS), or their mixtures) were also decomposed using the cell method at 700 °C with autogenic pressures at approximately 1000 psi. PET and HDPE produced completely spherical carbons with diameters of 3–5 μm. LDPE yielded 2–8 μm egglike or semispherical carbon particles alongside some spheres. Polydispersed carbon microspheres (4–10 μm) with a soft surface were produced from PS. The mixture of various plastics with different ratios also yielded similar spherical products. The products were more than 99% carbon. The solid yield of the product was 30–55% with 40% being characteristic. Prolonged reaction times did not affect the size and shape of the products but slightly improved the graphitic order. The benefit of such a process would be not only the production of the final carbon product but also the treatment of plastic wastes which are currently a global environmental burden. Furthermore, the carbon spheres produced through another similar experiment were tested as anodes in lithium ion batteries.[65] A steady reversible capacity of approximately 240 mA h g^{-1} for hundreds of cycles was achieved. If high temperature heat treatment was exerted on the carbon prior to anode testing, it not only increased the graphitic order of the products but also radically decreased the first-cycle irreversible capacity loss of the cells from 60 to 20%.

The possibilities of the various materials which could be treated inside such an autoclave cell are endless. Various core–shell particles with metals such as superconducting tin core–shells and ZnO@C have been produced.[66,67] As another example, a nickel-based organic compound (nickel acetylacetonate: $Ni(C_5H_7O_2)_2$) was also treated in the autogenic system.[68] As the temperatures increased, metallic nickel particles were formed by vapor nucleation and condensation. In zones with higher temperatures, the dissolution of the released carbon in the nickel particles took place. During cooling, the solubility of supersaturated particles decreased, and thus, the carbon was segregated by this "segregation flux". This segregation flux initiated carbon nanotube growth because of the lack of time to create an equilibrium structure. Meanwhile the carbon atoms diffused on the surface of the particles in order to reach the lowest energy state. If the cooling rate is

extremely slow, the most thermodynamically stable equilibrium structure, that is a sphere, will be formed. The resulting product had a Ni core surrounded by graphitic carbon which showed typical ferromagnetic curves with a saturation magnetization of 23.5 emu g^{-1}. The elemental measurement of the Ni−C core−shell (NCCS) particle showed 42% carbon and 1% hydrogen. The core sizes were 30−180 nm and covered by a 15 nm carbon layer. The BET surface area of the shell−core structure was 75.6 m^2 g^{-1}.

More recently, spherical carbons were produced in the range of 500−800 °C (mostly at 600 °C) and a pressure of 20 MPa from cyclic hydrocarbons such as toluene, benzene, xylene, and naphthalene.[69] The resulting diameters ranged from 1 to 12 μm. The concentric carbon layers of the spheres were not entirely graphitized. Some spheres had docked into one another in the course of their growth to build necklacelike structures. It was postulated that the spheres were in solid state before they became linked and that the growth process resulting in the linkage continued due to the deposition of additional gases after the contact. Spheres synthesized from different starting feeds had different sizes, but were similar in their formation and properties. In another article the same team of researchers reported that the necklace formation is not always mechanically strong and can be broken to separate the spheres.[70] There are numerous graphitized layer edges on the spheres where peripheral atoms have unsaturated bonds. Elsewhere a polytetrafluoroethylene (PTFE), carbon dioxide, and magnesium metal autoclave system at 650 °C has been shown to yield microspheres in chains.[71]

2.2. Prolate spheroids. A prolate spheroid also known as an ellipsoid, olivary, or rugby-ball is a shape obtained by the rotation of an ellipse about its longer principal axis. There are a limited number of studies which have recently observed the emergence of such carbon products in HTHP systems.

In one study, discarded oil alongside supercritical carbon dioxide was evaluated in a HTHP system.[72] When oil was heated in a supercritical carbon dioxide environment, small molecules and free radicals were formed which then combined to form other molecules such as pentagonal and hexagonal rings (see Figure 5). The increase of temperature and duration led to the condensation of molecules and the formation of graphene clusters with low levels of graphitization. At 500 °C most of the formed solids had random geometries. At slightly higher temperatures non uniform prolate spheroids were seen alongside spheres. When more dry ice was initially used in the closed cell, the autogenic pressures increased, and more spheres were seen (as opposed to other structures). With a fixed amount of precursors, the increase of temperatures not only increased the overall solid yield, but also increased the carbon sphere fraction. Under the treatment conditions of 550−650 °C and a duration of 3 h, carbon microspheres with diameters of 1−10 μm were formed. Waste oil or salad oil provided comparable results. Spheres with low BET surface areas and a multilayer structure could be obtained with subsequent vacuum annealing. With the increase of annealing temperature more small molecules evaporated and interlayer distances increased.

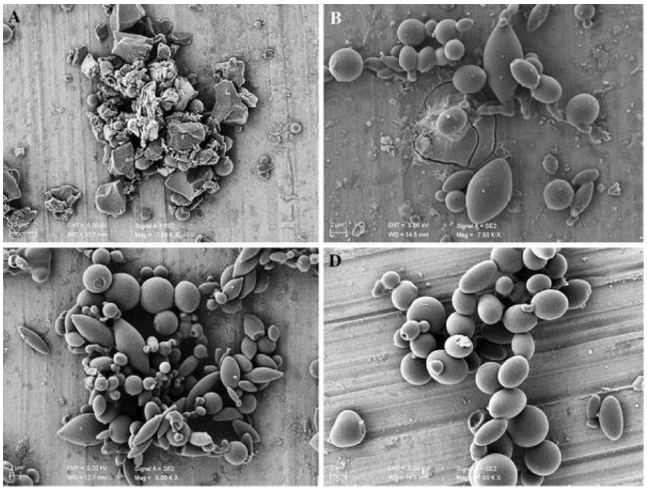

Figure 5. Evolution of products from the treatment of 6 mL of discarded oil and 14 g of dry ice in a closed 22.9 mL autoclave at (a) 500 °C, (b) 530 °C, (c) 550 °C, and (d) 650 °C.[72]

Elsewhere, when refined corn oil was heated in a closed autoclave system, the resulting solid was in the form of smooth, monodisperesd prolate spheroids with polar and equatorial diameters of 3 and 1.5 μm, respectively.[73] The majority of corn oil is composed of triglycerides with a chemical formula of RCOO−CH_2CH(−OOCR′)CH_2−OOCR″, where R, R′, and R″ are long alkyl chains. It was proposed that discotic nanocrystalline graphite units consisting of 6−7 stacked grapheme sheets form the initial nuclei which led to the formation of the American-football-shaped solids with time. It was found through solid-state ^{13}C NMR that the solid was mostly aromatic (<1% aliphatic) carbon with =114 carbons/cluster. About 11% of the material within the autoclave was oxygen evolving out of the liquid, and therefore, the researchers proposed that the existence of oxygen had a direct relation with the formation of the spheroids. Mass spectroscopy (MS) measurements showed that, while heating up to 170 °C, the ester bonds broke. At T < 270 °C molecules and radicals with 5 or less carbons were seen, while at 300 °C thermolysis of the oil resulted in compounds such as acrolein. Beyond this, up to 660 °C, the mass spectra remained rather unchanged. At higher temperatures large species were no longer detected and molecules with one to three carbons remained. The internal pressure of the system gradually increased and reached the final value of 4.2 MPa. In another research paper using olive oil in a closed reaction cell at 700 °C for 20 min, the team of researchers explained that the fluid/fluid interface during the reaction is of importance.[74] The two liquid phases are those of the carbonaceous mesophase and the noncondensed phases of the dissociated products at the autogenerated pressure inside the autoclave. The rugby ball shape is thought to be the shape which minimizes the energy of the C−H−O system. This is thought to be the case due to the hydrophiles which produce the anisotropy to the surface energy. Thus the sphere morphology is altered to the spheroid. The CO and CO_2 gases which are formed during the experiment due to the existence of oxygen are thought to interfere and/or cross link the formed discotic graphitic nanocrystallites due to their divalency. Compared to round spheres produced by the same research team in other experiments, the olivary (rugby shaped) spheroids had smaller sp_2-type clusters, a preferential ordering inside the clusters along the plane perpendicular to the graphitic plane, and more disorders. More recently, Gedanken's research team has added to previous information on the production of olivary products from carbon sources under pressure.[75] In their experiments a range of organics was used as the feedstock. Mesitylene, stearic acid, oleic acid, linoleic acid, methyl-3-butenoate, methyl butyrate, octadecane, octadecene,

octane, octene, and acrolein were heated to 700 °C at a heating rate of 40 °C min^{-1} and kept under their autogenic pressures for 10 min. In the early stages of carbonization, a crude sheetlike structure was first formed. The carbon atoms had delocalized electrons and were organized preferentially in aromatic rings. The biggest disklike structure was thought to first form the center, followed by smaller disks which stick to it along its growth. Rodlike structures present in the system introduce a directional preference along the quatorial axis. The polar and equatorial diameters of the final spheroidal product obtained from octadecene, octene, and methyl-3-butenoate were 2−4 μm and 4−6 μm, respectively. More than 98% of the product was composed of carbon, as shown in the C, H, N, S, O chemical analysis. Changes in the heating rate and heating time were found to cause no alteration in the morphology of the product. In contrast to the claims of Pol et al., the researchers observed that oxygen was not essential for the growth of the prolate spheroid structure. Rather, one double bond is the prerequisite for their production. If there was no double bond in the precursor, i.e. the precursor was saturated, prolate spheroid shapes were not observed regardless of oxygen content, heating rate, and heating time.

When using carbohydrates including glucose, sucrose, and starch as the precursor, Zheng et al. realized that alcoholic solvents act as a structure-directing agent which provokes the carbon spheres to reform as spheroids.[76] Their proposed mechanism stated that at temperatures below 200 °C the carbohydrates hydrolyze and polymerize to form colloidal nanospheres with functional surfaces. With the increase of temperature, the speed of the sphere formation will increase and they will self-assemble into aggregates due to surface tension. The alcohol then polymerizes and absorbs some exposed surfaces of the colloidal spheres. These sections are hindered in growth while the rest of the colloid continues to grow. In the higher range of the temperature, the alcohols or oligomers are carbonized and cover the aggregating colloids. These aggregates finally fuse to form spheroidal materials. At 550 °C the fusion is complete. Holding times of 6−12 h were more specifically tested, whereas prolonging the holding time to 48 h tended to increase the size of the product. In the presence of different alcohols, different spheroidal aggregates were produced, while in the absence of alcohol, spheres were formed. No clear difference was seen among the processing of glucose, sucrose, or starch. The resulting products had hydroxyl and carboxyl groups, and their polar and equatorial diameters were 5−8 μm and 2−3 μm, respectively. The researchers concluded that carbohydrates, alcohols, and H_2O are essential factors for the fabrication of carbon spheroids. The carbohydrates and alcohols control the shape and aspect ratio of the spheroidal product. For example, at a given amount of carbohydrates, the increase of the alcohol concentration within a range yields spheroids with larger diameters.

Elsewhere, manganese acetate tetrahydrate and absolute ethanol were treated in a closed autoclave system at 600 °C (10 °C min^{-1}temperate rise) for 12 h to produce olivary carbons.[77] No spheroids were seen below 500 °C. At the optimum temperature of 600 °C, 2 h is not enough to form the olivaries, while 24 h is too long to maintain the desired morphology. The evolution of the spheroid product with time can be seen in Figure 6. The researchers proposed that the $Mn(CH_3COO)_2$·OO_2O initially decomposes into $MnCO_3$, water and carbon fragments, while the ethanol is transformed into various sized carbon spheres at higher temperatures. As the pressure builds

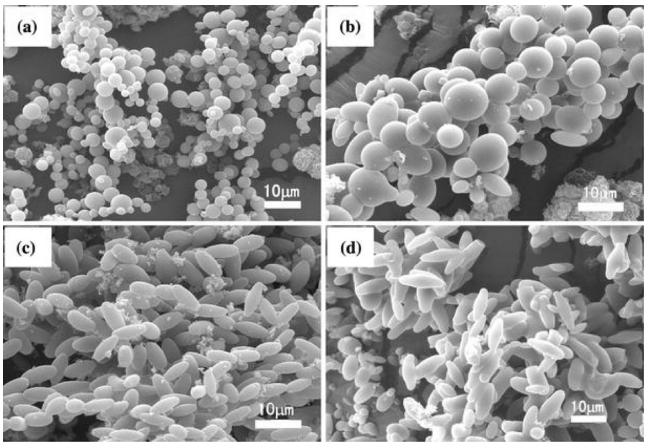

Figure 6. The evolution of spheroid particles formed from the pyrolysis of ethanol maintained at 600 °C for different reaction times: (a) 2 h, (b) 5 h, (c) 12 h (optimum), and (d) 24 h.[77]

up, two smaller sized spheres, adhere to the opposite poles of a big one with the assistance of the previously mentioned carbon fragments, fuse, and grow into an olivary spheroid. Figure 7

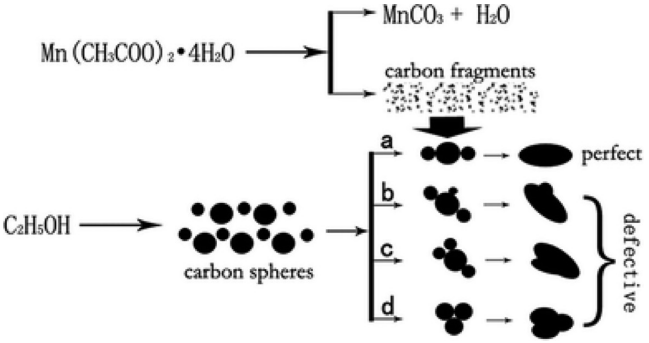

Figure 7. Possible formation process of the olivary particle.[77]

shows the proposed mechanism. An augmentation in the manganese acetate content increased the amount of carbon fragments and number of spheroids while further unifying the morphology. The products had an estimated carbon content of above 90% and were 4−6 μm wide and 8−12 μm long. The olivary carbons were amorphous, had a large number of hydroxyl groups on the surface, had a low graphitic degree, and were predominantly smooth.

Copper foil has been shown to assist the growth of ellipsoidal carbon microparticles as well.[78] Acetone was used as the precursor, and the temperature was kept at 500 °C for 12 h. As a result olivaries 1.5−2 μm wide and 3−4.5 μm long were produced. It was observed that the Cu substrate, reaction temperature, and time were critical parameters which affected the appearance of the product. In such a system, temperatures under 550 °C did not lead to the full carbonization of acetone. In addition, if reaction times were less than 12 h, the products were classified as "imperfect" ellipsoidal carbon microparticles. Interestingly if instead of Cu other metallic foils such as Al or Cr were used, microspheres are obtained instead of ellipsoids. This was also the case if no foil was used. Another study by the same group observed that Ni metallic substrates also led to the production of microspheres, whereas if Zn foil was used, uneven ellipsoidal carbon particles were obtained.[79]

Another experiment which used a metallic catalyst and acetone as the carbon source resulted in olivary particles ~1.5−2 μm wide and ~3−4 μm long.[80] The synthesis of olivary particles was suggested to be a self-assembly process which is indirectly catalytic. This means that the catalyst does not operate on the formation of the spheroid itself, but rather, operates on the polyreaction to form the intermediate products which then self-assemble into ellipsoids. Prior to the closed-system pyrolysis at 600 °C for 12 h, a 30 min ultrasonication was carried out in order to increase the 2-allyl alcohol ratio. This was done so that the desired intermediate product which was a kind of polyhydroxyl alcohol with a carbon chain became more frequent. The ultrasonication was shown to affect the final product considerably. With increase of ultrasonication times so did the size of the ellipsoids. Under optimum conditions more than 90% of the product was in the olivary form, homogeneous in shape, and highly disordered. As for the temperature, below 500 °C no spheroids were seen, while at above 700 °C, the spheroid particles combined to form carbon fibers. Butanone was also tested in place of acetone successfully. Various catalysts, namely Mg, Ni, Fe, Cu, Zn, and Cd powder, were also examined. From these, Zn had the best performance, followed by Fe and Cd, while Mg, Ni, and Cu did not have any noticeable catalytic roles.

2.3. Nanotubes. Since their discovery in the early 1990s carbon nanotubes have become one of the most popular areas of research regarding carbon products.[81−89] Today several different methods have been established for their production. Nonetheless, HTHP systems have also been shown to produce CNTs.

Calderon Moreno et al observed that in a pressurized system of amorphous carbon and double distilled water, carbon atoms rearrange to form curved graphitic layers during hydrothermal treatment at 600−800 °C and 100 MPa.[90] The reordering of carbon bonds and rapid growth of carbon clusters and patches are induced by the reactivity and mobility of the hydrothermal fluid. These patches have a rather stable lattice and are rich in graphitic sp2-bonds. The higher the temperature, the faster the kinetics and the formation will be. At 600 °C, the multiwalls curl and overlap to produce carbon nanocells. These cells have outer and inner diameters of 15−100 nm and 10−80 nm respectively. Interconnecting branches which are shared by several cells hold together the walls of the cells which are made of 4−20 concentric layers with interlayer spacing of 3.3A°. Small amounts of amorphous carbon still remain after the process. Some nanotube-like structures with disordered lattices could also be observed near the edge of the amorphous particles. At a temperature of 800 °C, multiwalled carbon nanotubes with no defects are produced. These carbon nanotubes with 8−20 layers have outer diameters in the range of tens and lengths in the range of hundreds of nanometers. Their crystallinity is similar to, or higher than, nanotubes grown using evaporation methods. Calderon Moreno et al went on to state that the hydrothermal conditions provide a sort of catalytic effect due to the reactivity of the supercritical water.[91] Compared to the vapor phase in inert atmospheres, the hot pressurized water allows the graphitic sheets to grow, move, curl and reorganize bonds at lesser temperatures. This is because of the physical tendency to minimize the energy level and reduce the number of dangling bonds to reach a more stable structure.

Elsewhere, carbon dioxide was used as the carbon source and metallic Li as a reductant to synthesize CNTs at 500 °C and 700 atm for 10 h.[92] A typical experimental run used 8.0 g CO_2 and 0.5 g metallic Li so that excess CO_2 existed for lithium oxidation. Being above the critical point improved the electron transfer from CO_2 to Li due to the enhanced absorption of carbon dioxide on the surface of the lithium. The following reactions were thought to occur:

$$CO_2 + 4Li \rightarrow C(\text{graphite}) + 2Li_2O \quad (1)$$

$$CO_2 + Li_2O \rightarrow Li_2CO_3 \quad (2)$$

Free energy calculations showed that the reaction $3CO_2 + 4Li \rightarrow C$ (graphite) + $2Li_2CO_3$ is spontaneous ($\Delta G°$=-1.09 × 10$\hat{3}$ KJ/mol) making the production of CNTs possible. The total solid yield relative to the initial CO_2 was about 92.5%, from which CNTs accounted for 80% of the product while the rest were amorphous carbon and graphite. The interlayer spacing of the multiwalled CNTs was more than that of graphite: 3.40 Å as opposed to 3.35 Å. The nanotubes were hollow with diameter of about 55 nm and lengths longer than 1.5 μm. Higher temperatures such as 700 °C resulted in a better quality (higher crystallinity and longer lengths as much as 12 μm) at the expense of a reduction in yields. The interior surface of the cell did not have a significant catalytic effect on the products, as repeating the process within a copper cell also produced the same products. The replacement of Li with K or Na resulted in the production of large amounts of graphite and the absence of nanotubes. Autogenic cells with only dry ice (no metals) produced no solid products. However in another study, the use of acetone as the carbon source and sodium azide as the reductant interestingly showed that the capacity of the autoclave strongly influences the final morphology of the products.[93]

Another study to observe that alkali metals (Li or Na) act as the reductants to synthesize CNTs was performed at 600−750 °C under autogenic pressures for 10 h.[94] Lithium has a low mass and a relatively weak metallic bond which allow it to form nanodroplets more easily, inducing CNT growth. These droplets first absorb CO_2 gas and act as reductants, followed by the formation of nanotubes on the droplets. If two CNTs grow near each other, they wrap and form a double helical CNT in order to reduce the surface dangling bonds. This accounts for about 70% of the product. Some nanotubes have suffered corrosion and have become porous, while in others the corrosion process has resulted in a complete breakup of the CNT into smaller fragments. Although the use of lithium results in no bamboolike structures, all the nanotubes grown by using sodium as a reductant in the temperature range of 650−750 °C are bamboolike and have no metals encapsulated within them. With an increase of temperature, the diameters decrease and lengths increase.

The same group of researchers also tried using $NaBH_4$ as the reductant in a supercritical carbon dioxide cell.[95] As temperature rose to above 400 °C, $NaBH_4$ began to decompose and release hydrogen gas. The existence of CO, CO_2, and H_2 within the autoclave alongside the iron and nickel components of the stainless steel interior wall were thought to benefit the Fischer−Tropsch synthesis. The Fischer−Tropsch process generates liquid hydrocarbons through a collection of chemical reactions from a mixture of gases.[96−99] Initially the main products were amorphous carbon, and conventional CNTs started to emerge at temperatures of about 600 °C. As the temperature was further increased to 700 °C, Y-junction nanotubes with a bamboo-shaped, hexagonal graphite structure became the

prevalent product. Y-junction CNTs, which were not seen in systems using alkali metals as the reductant, consist of a longer stem and shorter branch which connect in the form of the letter Y. The nanotubes have closed tips not encapsulating any solid particles. Nearly parallel graphite atomic planes were seen which were well crystallized and aligned to the tube axis at the wall with a small angle of about 15°. The diameter and length of the CNTs were about 100 nm and >10 μm, respectively.

In a study by Qian's group, helically coiled carbon nanotubes with diameters of 50−100 nm were produced from ethyl ether precursors and metallic zinc particles at 700 °C and 12 h.[100] When the temperature of the system went beyond 550 °C, the ethyl ether vaporized, and a highly exothermic reaction on the surface of the metallic zinc powder caused the vaporization of the zinc itself. The zinc droplets which were formed reacted with ethyl ether to produce zinc oxide which then acted as a catalyst for the helically coiled CNTs. An intermediate carbon dimer was also produced simultaneously through thermal dehydrogenation and the deoxidization of ethyl ether by zinc.

The carbon dimer C_2 was thought to be effective in the CNT formation by adsorption onto the metallic particles and formation of carbon rings. About 80% of the product was helically coiled with many defects, while the rest were multiwalled carbon nanotubes. If temperatures were elevated to above 700 °C, the products transformed to carbon microspheres.

Ethanol has also been used with Mg in a closed autoclave system at 600 °C for 10 h for the production of CNTs.[101] The reaction within the cell was:

$$CH_3CH_2OH + Mg \rightarrow 2C + MgO + 3H_2 \quad (3)$$

Bamboo-shaped multiwall carbon nanotubes with a high yield of 80% were synthesized. The length of the CNTs varied from hundreds of nanometers to several micrometers, while the diameters were 30−100 nm. Y-junction nanotubes were also seen. Some compartmented layers existed between the walls, and many CNTs had open ends.

In another study aimed at CNT production, carbon dioxide was reacted with Mg in a closed autoclave and kept under its autogenic pressures at 1000 °C for 3 h.[102] The chemical reactions which take place within the cell are thought to be:[103]

$$Mg(g) + CO2(g) \rightarrow MgO(s) + CO(gas) \quad (4)$$

$$Mg(l) + CO(g) \rightarrow MgO(s) + C(graphite) \quad (5)$$

First, the reaction takes place in the homogeneous gas phase. As the temperature rises above the melting point of Mg (650 °C), a heterogeneous reaction on the surface of liquid magnesium ensues. The boiling point of Mg is 1090 °C, and the vapor pressure of magnesium at 1000 °C is 350 mmHg. The pressure of the cell was not measured directly but calculated to be approximately 10,000 bar at 1000 °C. The carbon dioxide within the cell is supercritical. In the initial stages, the temperature of the oven is 100 °C less than the temperatures within the cell, showing the exothermic nature of the process. The mass balance shows that due to the extreme temperature and pressure nearly 60% of the gases leak out during the experiment. The cell is removed from the oven and opened without any apparent pressure release. The resulting solid is treated with HCl in order to remove the MgO. The total yield of carbonaceous material relative to the initial CO_2 content is a bit more than 15%. About 10% of this material consists of carbon nanotubes with diameters and lengths of 30−40 nm and 500−600 nm, respectively, while 1−2% are nested fullerenes. Some noncrystalline, impure, elongated, and aggregated carbon rods can also be observed. The CNTs are highly crystalline with closed-end multiwalls. When Mg is not used within the system, no products are produced. The researchers stated that there is no evidence to show that the transition metals of the stainless steel cell catalyze or effect the formation of CNTs and nested fullerenes. There is other research which claims the opposite. The difference between the two claims may be in the different experimental setups (including the different precursors). For example, elsewhere ethanol has been employed inside a cylindrical stainless tube which acts as both a reactor and catalyst for the production of multiwall carbon nanotubes.[104] About 5 mL of ethanol with high purity was loaded inside the stainless steel tube, followed by a purge of inert argon gas, pressurization (typically between 5 and 10 atm), and subsequent sealing and heating. As the temperature was raised to 600−900 °C, the pressure within the chamber was kept constant by controlling the argon. The reaction was sustained for 0.5−2 h before the reactor was left to cool to room temperature. During the process ethanol breaks up, and carbon atoms are produced on the interior metallic surface via catalytic decomposition. Carbon atoms are thought to solvate and diffuse in the molten solvent to ultimately precipitate to form CNTs. The multiwall nanotube products are varied (bamboo-shaped, spiral, Y-shaped, W-shaped) and highly graphitized. If the pressure is kept lower, the quantity and the graphitization degree of the products are reduced.

In general it has been claimed that carbonates or oxalates (such as magnesium carbonate) which can decompose to give off CO_2 gas at relatively low temperatures can be used alongside lithium in an autogenic system for the production of carbon nanotubes.[105] The magnesium carbonate system at 600 °C for 10 h produced CNTs (~75%) with an average length of 13 μm and diameter of 60 nm, graphite, and amorphous carbon. The structure of the CNTs is different from conventional carbon nanotubes. They are formed from short coaxial conical cylinder tubular graphite sheets which are aligned along the axis—and not parallel to it. Due to the length difference of the graphite sheets, the internal surface of the CNTs is coarse.

Composite nanotubes can also be obtained in HTHP systems. For example, highly crystalline and defect-free WC nanotubes were produced by heating of $W(CO)_6$ in the presence of Mg powder in an autogenic system at 900 °C for 3 h.[106] The products, which are straight, coiled, or zigzag in shape, have diameters of 30−70 nm and lengths of several micrometers. If sodium is used instead of magnesium, totally different morphological and crystallographic products are seen. The existence of Na resulted in the formation of Na_2WO_4. If $W(CO)_6$ is used without magnesium or sodium powder, a mixture of nanometric wirelike products composed of mainly WO_2, alongside WC, W_2C, and C are produced. The use of Mg is thus for the reason of its reactivity with oxygen and avoidance of WO_2. The researchers also concluded that the small reaction cell consisting of Fe, Co, Ni, or Cr had no catalytic effect. The next section of the review provides further examples of exotic materials which can be produced with the HTHP system.

2.4. Others. Aside from the above-mentioned carbon structures which are more frequently seen in the literature, there exists a wide spectrum of other carbonaceous materials which can be produced from different precursors.[107] In the late 1980s and early 1990s a variety of carbons with dispersed

molecules such as nickel, boron, iron, among others were produced by Naka, Hirano, and co-workers at temperatures and pressures no higher than 700 °C and 125 MPa, respectively.[108−114] Table S2 of the Supporting Information provides a summary of more recent studies with products which do not fit in the previous categories. Figures 8, 9, and 10 show some

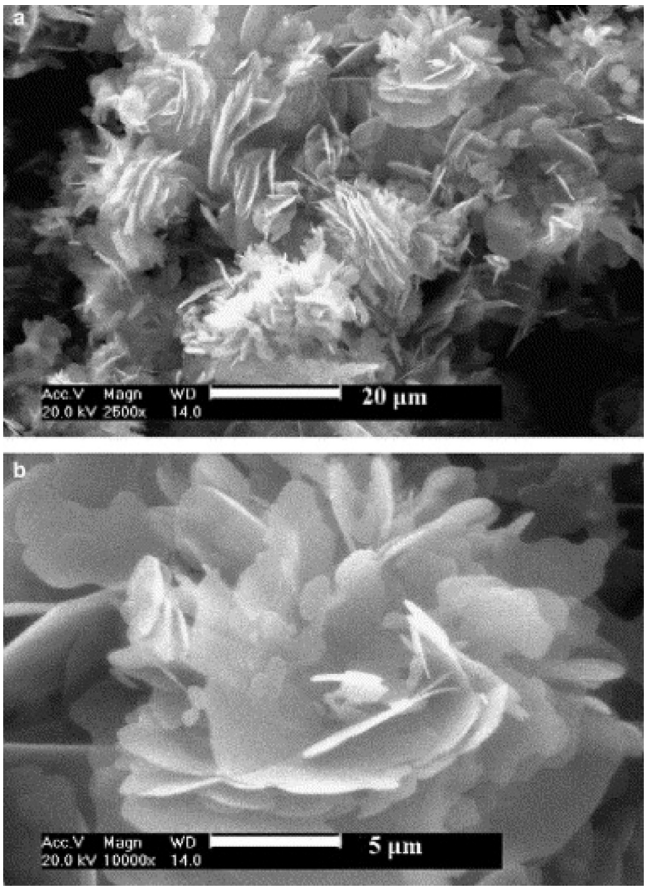

Figure 8. Flowerlike carbon materials.[122]

example images of the exotic products. Other mentionable examples of various HTHP studies are those which aim to modify the nanostructures of materials such as the hydrogenation of fullerenes. Fullerenes have been shown to react with hydrogen gas at high temperatures (400−600 °C) and pressures of 50−150 bar, forming hydrofullerides $C_{60}H_x$ and other compounds such as $C_{60}H_{36}$ and $C_{60}H_{18}$.[115−121]

3. DISCUSSION

As carbonization occurs, various gases such as hydrocarbons, carbon oxides, and hydrogen evolve from the decomposing

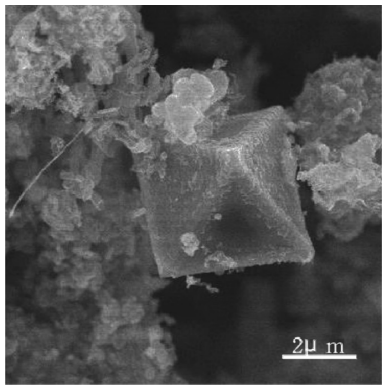

Figure 10. Octahedral diamond synthesized in the CO_2−Li system at 600 °C.[124]

solid. As gases emerge from the precursor, carbon atoms are lost from the solid phase. It is seen that under high pressures residues are obtained from precursors which would otherwise not provide any solid residue under atmospheric conditions. Generally, solid yields under pressure are higher than atmospheric yields. Additionally HTHP conditions alter the solubility, viscosity, density, and phase separation of molecules within the reactor. This in turn influences the graphitization behavior of the resulting carbons. Inagaki et al.'s general classification of carbonization under pressure still holds.[32] The only modification to the above classification that is required is the replacement of the word "hydrothermal" with "solvothermal". That is because hydrothermal processes are those which employ water as a solvent, whereas many HTHP studies exist which use other solvents such as alcohols. So the general categorization of studies pertaining to HTHP systems is expressed as follows:

(i) carbonization of precursors in the atmosphere of their decomposition gases under pressure
(ii) carbonization under solvothermal conditions
(iii) reduction of CO_2 under pressure

The biggest hindrance of implementing the use of HTHP systems on a large scale is the high price of the equipment needed for such systems. Currently the price for a small high-pressure reactor unit 50−200 mL is much higher than those operating at more moderate temperatures or pressures. Many companies do not even undertake the production of HTHP systems due to stringent safety requirements, technical feasibility, and other excessive costs such as the need for specialized alloys. Hence, with the consideration of the extreme prices for pressurized thermolysis systems, highly valuable products are needed in order to render the process economical. To date, none of the reviewed articles have shown enough economic potential to be tested at pilot-plant scale. Nonethe-

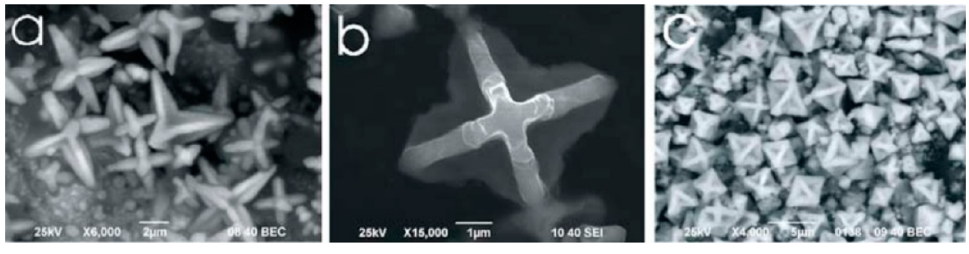

Figure 9. Starlike and other exotic materials from autogenic decomposition of ferrocene and water in different ratios.[123]

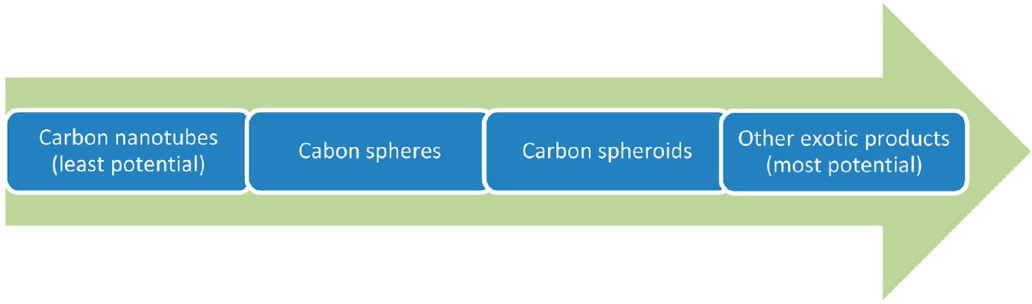

Figure 11. Future prospect for producing carbonaceous materials via HTHP systems.

less, years of research and scrutiny are needed. For now, the HTHP method can be primarily seen as a research tool for the exploration of unknown frontiers in material synthesis which can aid the pursuit of new and exotic forms of solid carbon-based materials. Once promising new materials have been identified, new and less expensive avenues for their industrial production can be sought. Figure 11 shows the future potential of producing carbonaceous materials with HTHP systems based on current knowledge. It should also be noted that systems operating under autogenic pressures will be less expensive than those requiring the provision of large pressures via external force or compressed gas.

Carbon nanotubes are currently produced in large amounts across the globe with a variety of different methods. From among the methods the CVD method[125,126] has been shown to be the best-suited for industrial large-scale production. By taking a look at various CNT production methods, we can see that the HTHP method currently falls short in various aspects such as the quality of the products and continuity of the process.[127]

Carbon spheres have also been produced by using various methods,[128,129] and studies have gone as far as pilot-plant scale analysis.[130] The research regarding carbon spheres shows many possible methods for obtaining such products, many of which operate at more desirable temperatures and pressure conditions. Thus, although the HTHP method can produce good spherical products, there are other methods which look more promising and less expensive. Unless the spheres prepared under pressure exhibit properties which other carbon spheres do not have, the pressurized, high-temperature production of carbon spheres does not seem to be economically attractive.

Unlike carbon spheres, carbon ellipsoids (spheroids) have not been widely produced with other conventional methods. The studies pertaining to this type of product are very few and far between. In fact, in the past decade the number of studies concerned with the production of solid carbon prolate ellipsoids does not go beyond a single digit. One reason may be due to the lack of applications shown for such products. Nonetheless, nonspherical particles such as olivaries may be more attractive in the future than their spherical counterparts due to a lower symmetry. Since HTHP systems are the leading method for synthesizing olivaries so far, they have been placed higher up the hierarchy as shown in Figure 11.

Exotic carbonaceous materials seem to be the most promising area of research for pressurized high temperature systems. This is due to the opportunities brought about by the seemingly endless possibilities of precursors and produced nanostructures. The HTHP method allows for the synthesis of products which have rarely been seen before—both carbonaceous[131] and non-carbonaceous.[132] The growth of other valuable products such as large-size diamonds are also of interest.[124] If any of these exotic materials show high added value, then there is a possibility that the large capital costs for a HTHP system could be overcome.

4. CONCLUSION

Reactions under high temperatures and pressures have been investigated for more than 5 decades. In recent years they have been investigated once more, with the objective of obtaining higher yields of unique solid products. Thus far, research has shown the possibility of producing various products under pressure including carbons spheres, prolate spheroids, nanotubes, and other exotics. A summary of the literature is provided. In particular the literature pertaining to the production of carbon ellipsoids has been collected for the first time. From among the various products of HTHP, the exotic carbon materials seem to have the most promising future, followed by the carbon spheroids. However, due to the existence of more feasible methods, the industrial production of carbon spheres and nanotubes via the HTHP method does not seem viable for the time being.

■ ASSOCIATED CONTENT

Supporting Information

Examples of studies not fitting the constraints of this review in Table S1, as well as a list of various exotic products produced from high pressure and high temperature systems in Table S2. This material is available free of charge via the Internet at http://pubs.acs.org.

■ AUTHOR INFORMATION

Corresponding Author

*E-mail: kemckayg@ust.hk. Telephone: (852) 2358 8412, Fax: (852) 2358 0054.

Notes

The authors declare no competing financial interest.

■ ACKNOWLEDGMENTS

We thank the staff at the Materials Characterisation and Preparation Facility at the Hong Kong University of Science and Technology for their assistance.

■ REFERENCES

(1) Inagaki, M. *New Carbons - Control of Structure and Functions*; Elsevier Press: Amsterdam, 2000.

(2) Inagaki, M.; Feiyu, K. *Carbon Materials Science and Engineering - From Fundamentals to Applications*; Tsinghua University Press: Beijing, 2006.

(3) Bundy, F. P.; Hall, H. T.; Strong, H. M.; Wentorf, R. H., Jr Man-made diamonds. *Nature* **1955**, *176*, 51−55.
(4) Kinney, C. R.; Nunn, R. C.; Walker, P. L. Carbonization of anthracene and graphitization of anthracene carbons. *Ind. Eng. Chem.* **1957**, *49*, 880−884.
(5) Marsh, H. Carbonization and liquid-crystal (mesophase) development: Part 1. The significance of the mesophase during carbonization of coking coals. *Fuel* **1973**, *52*, 205−212.
(6) Marsh, H.; Foster, J. M.; Hermon, G.; Iley, M. Enhanced graphitisation of fluorene and carbazole - A study of mesophase formation. *Carbon* **1973**, *11*, 425−426.
(7) Marsh, H.; Foster, J. M.; Hermon, G.; Iley, M. Carbonization and liquid-crystal (mesophase) development. Part 2. Co-carbonization of aromatic and organic dye compounds, and influence of inerts. *Fuel* **1973**, *52*, 234−242.
(8) Marsh, H.; Foster, J. M.; Hermon, G.; Iley, M.; Melvin, J. N. Carbonization and liquid-crystal (mesophase) development. Part 3. Co-carbonization of aromatic and heterocyclic compounds containing oxygen, nitrogen and sulphur. *Fuel* **1973**, *52*, 243−252.
(9) Goodarzi, F.; Hermon, G.; Iley, M.; Marsh, H. Carbonization and liquid-crystal (mesophase) development. 6. Effect of pre-oxidation of vitrinites upon coking properties. *Fuel* **1975**, *54*, 105−112.
(10) Goodarzi, F.; Marsh, H. Optical properties of carbon (HTT 673 to 873 K) from pre-oxidized vitrinites carbonized under pressures of about 200 MPa. *Fuel* **1980**, *59*, 268−269.
(11) Goodarzi, F.; Marsh, H. Retention of plant call structures in carbons (HTT 873 K) from pre-oxidized vitrinites carbonized under pressures of about 200 MPa. *Fuel* **1980**, *59*, 269−271.
(12) Bratek, K.; Marsh, H. Carbonizations under pressure of chloroformsoluble material of coking vitrinite. *Fuel* **1980**, *59*, 339−342.
(13) Forrest, M. A.; Marsh, H. The carbonization of blends of pitches and resins to produce anisotropic carbon and the effects of pressure. *J. Mater. Sci.* **1983**, *18*, 991−997.
(14) Green, P. D.; Edwards, I. A. S.; Marsh, H.; Thomas, K. M.; Watson, R. F. Coal thermoplasticity and coke structure as related to gasification. Effect of inorganic additives on high pressure dilatometric properties and reactivity towards hydrogen. *Fuel* **1988**, *67*, 389−395.
(15) Forrest, M. A.; Marsh, H. The effects of pressure on the carbonization of pitch and pitch/carbon fibre composites. *J. Mater. Sci.* **1983**, *18*, 978−990.
(16) Marsh, H.; Dachille, F.; Melvin, J.; Al, E. The carbonisation of anthracene and biphenyl under pressures of 300 MNm^{-2} (3 kbar). *Carbon* **1971**, *9*, 159−177.
(17) Wall, T. F.; Yu, J.; Wu, H.; Liu, G.; Lucas, J. A.; Harris, D. Effect of pressure on ash formation during pulverised coal combustion and gasification. *Prepr. Pap.—Am. Chem. Soc., Div. Fuel Chem.* **2002**, *47*, 801−806.
(18) Yu, J.; Harris, D.; Lucas, J.; Roberts, D.; Wu, H.; Wall, T. Effect of pressure on char formation during pyrolysis of pulverized coal. *Energy Fuels* **2004**, *18*, 1346−1353.
(19) Ajilkumar, A.; Shet, U. S. P.; Sundararajan, T. Numerical simulation of pressure effects on the gasification of australian and indian coals in a tubular gasifier. *Heat Transfer Eng.* **2010**, *31*, 495−508.
(20) Lee, C. W.; Jenkins, R. G.; Schobert, H. H. Mechanisms and kinetics of rapid, elevated pressure pyrolysis of Illinois No. 6 bituminous coal. *Energy Fuels* **1991**, *5*, 547−555.
(21) Landais, P.; Michels, R.; Poty, B.; Monthioux, M. Pyrolysis of organic matter in cold-seal pressure autoclaves. Experimental approach and applications. *J. Anal. Appl. Pyrolysis* **1989**, *16*, 103−115.
(22) Tamhankar, S. S.; Sears, J. T.; Wen, C. Y. Coal pyrolysis at high temperatures and pressures. *Fuel* **1984**, *63*, 1230−1235.
(23) Van Heek, K. H. *Druckpyrolyse Von Steinkohlen (Pressure Pyrolysis of Coal, Engl. Transl.)*; VDI-Forschungsheft, Vol. *612*; VDI-Verlag: Germany, 1982.
(24) Noda, T.; Kato, H. Heat treatment of carbon under high pressure. *Carbon* **1965**, *3*, 289−297.
(25) Beyssac, O.; Brunet, F.; Petitet, J.-P.; Goffé, B.; Rouzaud, J.-N. Experimental study of the microtextural and structural transformations of carbonaceous materials under pressure and temperature. *Eur. J. Mineral.* **2003**, *15*, 937−951.
(26) Sun, L.; Zhang, Y.; Li, H. Research on carbonization mechanism of coal-tar pitch under high pressure. *Mech. Mater. Eng. Sci. Exp.* **2003**, 608−611.
(27) Krebs, V.; Elalaoui, M.; Mareche, J. F.; Furdin, G.; Bertau, R. Carbonization of coal-tar pitch under controlled atmosphere - Part I: Effect of temperature and pressure on the structural evolution of the formed green coke. *Carbon* **1995**, *33*, 645−651.
(28) Gudiyella, S.; Brezinsky, K. The high pressure study of *n*-propylbenzene pyrolysis. *Proc. Combust. Inst.* **2013**, *34*, 1767−1774.
(29) Garner, S.; Sivaramakrishnan, R.; Brezinsky, K. The high-pressure pyrolysis of saturated and unsaturated C7 hydrocarbons. *Proc. Combust. Inst.* **2009**, *32*, 461−467.
(30) Gudiyella, S.; Brezinsky, K. High pressure study of *n*-propylbenzene oxidation. *Combust. Flame* **2012**, *159*, 940−958.
(31) Gudiyella, S.; Malewicki, T.; Comandini, A.; Brezinsky, K. High pressure study of *m*-xylene oxidation. *Combust. Flame* **2011**, *158*, 687−704.
(32) Inagaki, M.; Park, K. C.; Endo, M. Carbonization under pressure. *New Carbon Mater.* **2010**, *25*, 409−420.
(33) Inagaki, M.; Kuroda, K.; Sakai, M. Formation of carbon spherules from polyethylene under pressure. *High Temp. - High Pressures* **1981**, *13*, 207−213.
(34) Hishiyama, Y.; Yoshida, A.; Inagaki, M. Microstructures of carbon spherules. *Carbon* **1982**, *20*, 79−84.
(35) Inagaki, M.; Kuroda, K.; Sakai, M. Pressure carbonization of polyethylene-polyvinylchloride mixtures. *Carbon* **1983**, *21*, 231−235.
(36) Inagaki, M.; Kuroda, K.; Inoue, N.; Sakai, M. Conditions for carbon spherule formation under pressure. *Carbon* **1984**, *22*, 617−619.
(37) Inagaki, M.; Ishihara, M.; Naka, M. Mesophase formation during carbonization under pressure. *High Temp. - High Pressures* **1976**, *8*, 279−291.
(38) Inagaki, M.; Washiyama, M.; Sakai, M. Production of carbon spherules and their graphitization. *Carbon* **1988**, *26*, 169−172.
(39) Washiyama, M.; Sakai, M.; Inagaki, M. Formation of carbon spherules by pressure carbonization: Relation to molecular structure of precursor. *Carbon* **1988**, *26*, 303−307.
(40) Chemii, W. Novel methods for CO_2 remediation: Production of carbon nanomaterials. *Przem. Chem.* **2012**, *91*, 1726−1732.
(41) Pol, V. G.; Pol, S. V.; Gedanken, A. Dry autoclaving for the nanofabrication of sulfides, selenides, borides, phosphides, nitrides, carbides, and oxides: Review. *Adv. Mater.* **2011**, *23*, 1179−1190.
(42) Mohamed, A. R.; Mohammadi, M.; Darzi, G. N. Preparation of carbon molecular sieve from lignocellulosic biomass: A review. *Renewable Sustainable Energy Rev.* **2010**, *14*, 1591−1599.
(43) Inagaki, M.; Orikasa, H.; Morishita, T. Morphology and pore control in carbon materials via templating. *RSC Adv.* **2011**, *1*, 1620−1640.
(44) Yazdi, S. K.; Masoudi Soltani, S.; Hosseini, S. An investigation into the optimum carbonization conditions for the production of porous carbon from a solid waste. *Adv. Mater. Res.* **2012**, *587*, 88−92.
(45) Reza, M. T.; Lynam, J. G.; Uddin, M. H.; Coronella, C. J. Hydrothermal carbonization: Fate of inorganics. *Biomass Bioenergy* **2013**, *49*, 86−94.
(46) Liu, Z.; Quek, A.; Kent Hoekman, S.; Balasubramanian, R. Production of solid biochar fuel from waste biomass by hydrothermal carbonization. *Fuel* **2013**, *103*, 943−949.
(47) Becker, R.; Dorgerloh, U.; Helmis, M.; Mumme, J.; Diakité, M.; Nehls, I. Hydrothermally carbonized plant materials: Patterns of volatile organic compounds detected by gas chromatography. *Bioresour. Technol.* **2013**, *130*, 621−628.
(48) Funke, A.; Ziegler, F. Hydrothermal carbonization of biomass: A summary and discussion of chemical mechanisms for process engineering. *Biofuels, Bioprod. Biorefin.* **2010**, *4*, 160−177.

(49) Hu, B.; Wang, K.; Wu, L.; Yu, S.-H.; Antonietti, M.; Titirici, M.-M. Engineering carbon materials from the hydrothermal carbonization process of biomass. *Adv. Mater.* **2010**, *22*, 813−828.
(50) Worasuwannarak, N.; Potisri, P.; Tanthapanichakoon, W. Upgrading of biomass by carbonization in hot compressed water. *Songklanakarin J. Sci. Technol.* **2006**, *28*, 1049−1057.
(51) Davydov, V. A.; Rakhmanina, A. V; Boudou, J.-P.; Thorel, A.; Allouchi, H.; Agafonov, V. Nanosized carbon forms in the processes of pressure-temperature-induced transformations of hydrocarbons. *Carbon* **2006**, *44*, 2015−2020.
(52) Murata, K.; Sato, K.; Sakata, Y. Effect of pressure on thermal degradation of polyethylene. *J. Anal. Appl. Pyrolysis* **2004**, *71*, 569−589.
(53) Hirano, S.-I.; Ozawa, M.; Naka, S. Formation of non-graphitizable isotropic spherulitic carbon from poly-divinylbenzene by pressure pyrolysis. *J. Mater. Sci.* **1981**, *16*, 1989−1993.
(54) Ayache, J.; Oberlin, A.; Inagaki, M. Mechanism of carbonization under pressure, part I: Influence of aromaticity (polyethylene and anthracene). *Carbon* **1990**, *28*, 337−351.
(55) Ayache, J.; Oberlin, A.; Inagaki, M. Mechanism of carbonization under pressure, part II: Influence of impurities. *Carbon* **1990**, *28*, 353−362.
(56) Zhengsong, L.; Qianwang, C.; Jin, G.; Yufeng, Z. Preparation of carbon spheres consisting of amorphous carbon cores and graphene shells. *Carbon* **2004**, *42*, 229−232.
(57) Lou, Z.; Chen, C.; Zhao, D.; Luo, S.; Li, Z. Large-scale synthesis of carbon spheres by reduction of supercritical CO_2 with metallic calcium. *Chem. Phys. Lett.* **2006**, *421*, 584−588.
(58) Wei, L.; Yan, N.; Chen, Q. Converting poly(ethylene terephthalate) waste into carbon microspheres in a supercritical CO_2 system. *Environ. Sci. Technol.* **2011**, *45*, 534−9.
(59) Pol, V. G.; Pol, S. V.; Calderon Moreno, J. M.; Gedanken, A. High yield one-step synthesis of carbon spheres produced by dissociating individual hydrocarbons at their autogenic pressure at low temperatures. *Carbon* **2006**, *44*, 3285−3292.
(60) Jin, Y. Z.; Gao, C.; Hsu, W. K.; Zhu, Y.; Huczko, A.; Bystrzejewski, M.; Roe, M.; Lee, C. Y.; Acquah, S.; Kroto, H.; Walton, D. R. M. Large-scale synthesis and characterization of carbon spheres prepared by direct pyrolysis of hydrocarbons. *Carbon* **2005**, *43*, 1944−1953.
(61) Zheng, M.; Liu, Y.; Xiao, Y.; Zhu, Y.; Guan, Q.; Yuan, D.; Zhang, J. An easy catalyst-free hydrothermal method to prepare monodisperse carbon microspheres on a large scale. *J. Phys. Chem. C* **2009**, *113*, 8455−8459.
(62) Pol, V. G.; Motiei, M.; Gedanken, A.; Calderon-Moreno, J.; Yoshimura, M. Carbon spherules: Synthesis, properties and mechanistic elucidation. *Carbon* **2004**, *42*, 111−116.
(63) Pol, S. V; Pol, V. G.; Gedanken, A. Reactions under autogenic pressure at elevated temperature (RAPET) of various alkoxides: Formation of metals/metal oxides-carbon core-shell structures. *Chem.−Eur. J.* **2004**, *10*, 4467−4473.
(64) Pol, V. G.; Pol, S. V; Gofer, Y.; Calderon-Moreno, J.; Gedanken, A. Thermal decomposition of tetraethylorthosilicate (TEOS) produces silicon coated carbon spheres. *J. Mater. Chem.* **2004**, *14*, 966−969.
(65) Pol, V. G.; Thackeray, M. M. Spherical carbon particles and carbon nanotubes prepared by autogenic reactions: Evaluation as anodes in lithium electrochemical cells. *Energy Environ. Sci.* **2011**, *4*, 1904.
(66) Pol, V. G.; Thiyagarajan, P.; Acharya, S.; Ariga, K.; Felner, I. Superconducting nanocrystalline tin protected by carbon. *Langmuir* **2009**, *25*, 2582−2584.
(67) Zheng, M.; Liu, Y.; Zhao, S.; He, W.; Xiao, Y.; Yuan, D. Simple shape-controlled synthesis of carbon hollow structures. *Inorg. Chem.* **2010**, *49*, 8674−8683.
(68) Pol, S. V; Pol, V. G.; Frydman, A.; Churilov, G. N.; Gedanken, A. Fabrication and magnetic properties of Ni nanospheres encapsulated in a fullerene-like carbon. *J. Phys. Chem. B* **2005**, *109*, 9495−9498.
(69) Koprinarov, N.; Konstantinova, M. Peculiarities of carbon spheres obtained by hydrocarbon pyrolysis in hermetically closed container. *Physica E* **2012**, *44*, 1021−1023.
(70) Koprinarov, N.; Konstantinova, M. Preparation of carbon spheres by low-temperature pyrolysis of cyclic hydrocarbons. *J. Mater. Sci.* **2011**, *46*, 1494−1501.
(71) Wang, Q.; Cao, F.; Chen, Q. Formation of carbon microsphere chains by defluorination of PTFE in a magnesium and supercritical carbon dioxide system. *Green Chem.* **2005**, *7*, 733−736.
(72) Yu, B.; Kong, X.; Wei, L.; Chen, Q. Treatment of discarded oil in supercritical carbon dioxide for preparation of carbon microspheres. *J. Mater. Cycles Waste Manage.* **2011**, *13*, 298−304.
(73) Pol, V. G.; Calderon-Moreno, J. M.; Chupas, P. J.; Winans, R. E.; Thiyagarajan, P. Synthesis of monodispersed prolate spheroid shaped paramagnetic carbon. *Carbon* **2009**, *47*, 1050−1055.
(74) Pol, V. G.; Calderon-Moreno, J. M.; Thiyagarajan, P. Catalyst-Free, One-Step Synthesis of Olivary-Shaped Carbon from Olive Oil. *Ind. Eng. Chem. Res.* **2009**, *48*, 5691−5695.
(75) Gershi, H.; Gedanken, A.; Keppner, H.; Cohen, H. One-step synthesis of prolate spheroidal-shaped carbon produced by the thermolysis of octene under its autogenic pressure. *Carbon* **2011**, *49*, 1067−1074.
(76) Zheng, M.; Liu, Y.; Jiang, K.; Xiao, Y.; Yuan, D. Alcohol-assisted hydrothermal carbonization to fabricate spheroidal carbons with a tunable shape and aspect ratio. *Carbon* **2010**, *48*, 1224−1233.
(77) He, W.; Xiao, Y.; Cheng, J.; Wei, G.; Zhao, S.; Yi, G.; Liu, Y. Preparation and characterization of olivary carbon by pyrolysis of ethanol with the manganese acetate as promoter via solvothermal method. *J. Mater. Sci.* **2011**, *46*, 1844−1849.
(78) Ma, X.; Xu, F.; Du, Y.; Chen, L.; Zhang, Z. Copper substrate-assisted growth of ellipsoidal carbon microparticles. *Carbon* **2006**, *44*, 179−181.
(79) Ma, X.; Xu, F.; Chen, L.; Zhang, Y.; Zhang, Z.; Qian, J.; Qian, Y. Easy nickel substrate-assisted growth of uniform carbon microspheres and their spectroscopic properties. *Carbon* **2006**, *44*, 2861−2864.
(80) Luo, T.; Gao, L.; Liu, J.; Chen, L.; Shen, J.; Wang, L.; Qian, Y. Olivary Particles: Unique Carbon Microstructure Synthesized by Catalytic Pyrolysis of Acetone. *J. Phys. Chem. B* **2005**, *109*, 15272−15277.
(81) Golnabi, H. Carbon nanotube research developments in terms of published papers and patents, synthesis and production. *Sci. Iran.* **2012**, *19*, 2012−2022.
(82) Ansari, R.; Gholami, R.; Sahmani, S. On the dynamic stability of embedded single-walled carbon nanotubes including thermal environment effects. *Sci. Iran.* **2012**, *19*, 919−925.
(83) Shokrieh, M.; Rafiee, R. Development of a full range multi-scale model to obtain elastic properties of CNT/polymer composites. *Iran. Polym. J.* **2012**, *21*, 397−402.
(84) Dalali, N.; Ashouri, M.; Nakisa, S. Solid phase extraction based on modified multi-walled carbon nanotubes packed column for enrichment of copper and lead on-line incorporated with flame atomic absorption spectrometry. *J. Iran. Chem. Soc.* **2012**, *9*, 181−188.
(85) Hajibaba, A.; Naderi, G.; Ghoreishy, M.; Bakhshandeh, G.; Nouri, M. Effect of single-walled carbon nanotubes on morphology and mechanical properties of NBR/PVC blends. *Iran. Polym. J.* **2012**, *21*, 505−511.
(86) Alimardani, M.; Abbassi-Sourki, F.; Bakhshandeh, G. Preparation and characterization of carboxylated styrene butadiene rubber (XSBR)/multiwall carbon nanotubes (MWCNTs) nanocomposites. *Iran. Polym. J.* **2012**, *21*, 809−820.
(87) Zamani, M.; Fereidoon, A.; Sabet, A. Multi-walled carbon nanotube-filled polypropylene nanocomposites: high velocity impact response and mechanical properties. *Iran. Polym. J.* **2012**, *21*, 887−894.
(88) Rahimi-Razin, S.; Haddadi-Asl, V.; Salami-Kalajahi, M.; Behboodi-Sadabad, F.; Roghani-Mamaqani, H. Properties of matrix-grafted multi-walled carbon nanotube/poly(methyl methacrylate) nanocomposites synthesized by in situ reversible addition-fragmentation chain transfer polymerization. *J. Iran. Chem. Soc.* **2012**, *9*, 877−887.

(89) Nie, M.; Xia, H.; Wu, J. Preparation and characterization of poly(styrene-co-butyl acrylate)-encapsulated single-walled carbon nanotubes under ultrasonic irradiation. *Iran. Polym. J.* **2013**, *22*, 409−416.
(90) Calderon Moreno, J. M.; Swamy, S. S.; Fujino, T.; Yoshimura, M. Carbon nanocells and nanotubes grown in hydrothermal fluids. *Chem. Phys. Lett.* **2000**, *329*, 317−322.
(91) Calderon Moreno, J. M.; Fujino, T.; Yoshimura, M. Carbon nanocells grown in hydrothermal fluids. *Carbon* **2001**, *39*, 618−621.
(92) Zhengsong, L.; Qianwang, C.; Wei, W.; Yufeng, Z. Synthesis of carbon nanotubes by reduction of carbon dioxide with metallic lithium. *Carbon* **2003**, *41*, 3063−3067.
(93) Li, G.; Guo, C.; Sun, C.; Ju, Z.; Yang, L.; Xu, L.; Qian, Y. A Facile Approach for the Synthesis of Uniform Hollow Carbon Nanospheres. *J. Phys. Chem. C* **2008**, *112*, 1896−1900.
(94) Lou, Z.; Chen, C.; Chen, Q.; Gao, J. Formation of variously shaped carbon nanotubes in carbon dioxide-alkali metal (Li, Na) system. *Carbon* **2005**, *43*, 1104−1108.
(95) Lou, Z.; Chen, C.; Huang, H.; Zhao, D. Fabrication of Y-junction carbon nanotubes by reduction of carbon dioxide with sodium borohydride. *Diamond Relat. Mater.* **2006**, *15*, 1540−1543.
(96) Arabpour, M.; Rahimpour, M. R.; Iranshahi, D.; Raeissi, S. Evaluation of maximum gasoline production of Fischer-Tropsch synthesis reactions in GTL technology: A discretized approach. *J. Nat. Gas Sci. Eng.* **2012**, *9*, 209−219.
(97) Ghareghashi, A.; Ghader, S.; Hashemipour, H.; Moghadam, H. R. A comparison of co-current and counter-current modes for Fischer-Tropsch synthesis in two consecutive reactors of oxidative coupling of methane and Fischer−Tropsch. *J. Nat. Gas Sci. Eng.* **2013**, *14*, 1−16.
(98) Bayat, M.; Rahimpour, M. R. Simultaneous hydrogen injection and in-situ H_2O removal in a novel thermally coupled two-membrane reactor concept for Fischer-Tropsch synthesis in GTL technology. *J. Nat. Gas Sci. Eng.* **2012**, *9*, 73−85.
(99) Bayat, M.; Hamidi, M.; Dehghani, Z.; Rahimpour, M. R.; Shariati, A. Sorption-enhanced reaction process in Fischer-Tropsch synthesis for production of gasoline and hydrogen: Mathematical modeling. *J. Nat. Gas Sci. Eng.* **2013**, *14*, 225−237.
(100) Luo, T.; Liu, J.; Chen, L.; Zeng, S.; Qian, Y. Synthesis of helically coiled carbon nanotubes by reducing ethyl ether with metallic zinc. *Carbon* **2005**, *43*, 755−759.
(101) Liu, J.; Shao, M.; Chen, X.; Yu, W.; Liu, X.; Qian, Y. Large-Scale Synthesis of Carbon Nanotubes by an Ethanol Thermal Reduction Process. *J. Am. Chem. Soc.* **2003**, *125*, 8088−8089.
(102) Motiei, M.; Rosenfeld Hacohen, Y.; Calderon-Moreno, J.; Gedanken, A. Preparing carbon nanotubes and nested fullerenes from supercritical CO_2 by a chemical reaction. *J. Am. Chem. Soc.* **2001**, *123*, 8624−8625.
(103) Shafirovich, E. Y.; Goldshleger, U. I. Combustion of magnesium particles in CO_2/CO mixtures. *Combust. Sci. Technol.* **1992**, *84*, 33−43.
(104) Yang, H.; Mercier, P.; Wang, S. C.; Akins, D. L. High-pressure synthesis of carbon nanotubes with a variety of morphologies. *Chem. Phys. Lett.* **2005**, *416*, 18−21.
(105) Lou, Z.; Chen, C.; Chen, Q. Growth of conical carbon nanotubes by chemical reduction of $MgCO_3$. *J. Phys. Chem. B* **2005**, *109*, 10557−10560.
(106) Pol, S. V.; Pol, V. G.; Gedanken, A. Synthesis of WC nanotubes. *Adv. Mater.* **2006**, *18*, 2023−2027.
(107) Panchakarla, L. S.; Govindaraj, A. Carbon nanostructures and graphite-coated metal nanostructures obtained by pyrolysis of ruthenocene and ruthenocene-ferrocene mixtures. *Bull. Mater. Sci.* **2007**, *30*, 23−29.
(108) Yogo, T.; Suzuki, H.; Iwahara, H.; Naka, S.; Hirano, S.-I. Synthesis and properties of platinum-dispersed carbon by pressure pyrolysis of organoplatinum copolymer. *J. Mater. Sci.* **1991**, *26*, 1363−1367.
(109) Yogo, T.; Tanaka, H.; Naka, S.; Hirano, S.-I. Synthesis of boron-dispersed carbon by pressure pyrolysis of organoborane copolymer. *J. Mater. Sci.* **1990**, *25*, 1719−1723.
(110) Yogo, T.; Yokoyama, H.; Naka, S.; Hirano, S.-I. Synthesis of cementite-dispersed carbons by pressure pyrolysis of organoiron copolymers. *J. Mater. Sci.* **1986**, *21*, 2571−2576.
(111) Hirano, S.-I.; Yogo, T.; Kikuta, K.; Naka, S. Synthesis and properties of carbons dispersed with Fe-Co alloy by pressure pyrolysis of organoiron-organocobalt copolymer. *J. Mater. Sci.* **1986**, *21*, 1951−1955.
(112) Pogo, T.; Tamura, E.; Naka, S.; Hirano, S.-I. Synthesis and properties of nickel-dispersed carbons by pressure pyrolysis of nickelocene-divinylbenzene. *J. Mater. Sci.* **1986**, *21*, 941−946.
(113) Hirano, S.-I.; Yogo, T.; Suzuki, H.; Naka, S. Synthesis of iron-dispersed carbons by pressure pyrolysis of divinylbenzene-vinylferrocene copolymer. *J. Mater. Sci.* **1983**, *18*, 2811−2816.
(114) Yogo, T.; Naka, S.; Hirano, S.-I. Synthesis and properties of magnetite-dispersed carbon by pressure pyrolysis of divinylbenzene-vinylferrocene with water. *J. Mater. Sci.* **1989**, *24*, 2115−2119.
(115) Talyzin, A. V; Dzwilewski, A.; Sundqvist, B.; Tsybin, Y. O.; Purcell, J. M.; Marshall, A. G.; Shulga, Y. M.; McCammon, C.; Dubrovinsky, L. Hydrogenation of C_{60} at 2 GPa pressure and high temperature. *Chem. Phys.* **2006**, *325*, 445−451.
(116) Schur, D. V; Zaginaichenko, S. Y.; Savenko, A. F.; Bogolepov, V. A.; Anikina, N. S.; Zolotarenko, A. D.; Matysina, Z. A.; Veziroglu, T. N.; Skryabina, N. E. Experimental evaluation of total hydrogen capacity for fullerite C_{60}. *Int. J. Hydrogen Energy* **2011**, *36*, 1143−1151.
(117) Schur, D. V; Zaginaichenko, S.; Nejat Veziroglu, T. Peculiarities of hydrogenation of pentatomic carbon molecules in the frame of fullerene molecule C_{60}. *Int. J. Hydrogen Energy* **2008**, *33*, 3330−3345.
(118) Schur, D. V; Tarasov, B. P.; Shul'ga, Y. M.; Zaginaichenko, S. Y.; Matysina, Z. A.; Pomytkin, A. P. Hydrogen in fullerites. *Carbon* **2003**, *41*, 1331−1342.
(119) Peera, A. A.; Alemany, L. B.; Billups, W. E. Hydrogen storage in hydrofullerides. *Appl. Phys. A* **2004**, *78*, 995−1000.
(120) Shul'ga, Y. .; Tarasov, B. P.; Fokin, V. N.; Martynenko, V. M.; Schur, D. V; Volkov, G. A.; Rubtsov, V. I.; Krasochka, G. A.; Chapusheva, N. V; Shevchenko, V. V. Deuterofullerenes. *Carbon* **2003**, *41*, 1365−1368.
(121) Talyzin, A. V; Sundqvist, B.; Shulga, Y. M.; Peera, A. A.; Imus, P.; Billups, W. E. Gentle fragmentation of C_{60} by strong hydrogenation: A route to synthesizing new materials. *Chem. Phys. Lett.* **2004**, *400*, 112−116.
(122) Yong, X.; Yingliang, L.; Liqiang, C.; Dengsheng, Y.; Jingxian, Z.; Yunle, G.; Guanghui, S. Flower-like carbon materials prepared via a simple solvothermal route. *Carbon* **2006**, *44*, 1589−1591.
(123) Koprinarov, N.; Konstantinova, M. Shape diversity in particles obtained by low temperature pyrolysis of ferrocene. *Cryst. Res. Technol.* **2011**, *46*, 676−684.
(124) Lou, Z.; Chen, Q.; Zhang, Y.; Qian, Y.; Wang, W. Synthesis of large-size diamonds by reduction of dense carbon dioxide with alkali metals (K, Li). *J. Phys. Chem. B* **2004**, *108*, 4239−4241.
(125) Saeidi, M.; Vaezzadeh, M. Theoretical investigation of the growth rate of carbon nanotubes in chemical vapor deposition. *Iran. J. Sci. Technol., Trans. A: Sci.* **2011**, *35*, 29−32.
(126) Rashidi, A.; Mortazavi, Y.; Khodadadi, A. A.; Akbarnejad, M. M. The preparation of bamboo-structured carbon nanotubes with the controlled porosity by CVD of acetylene on Co-Mo/MCM-41. *Iran. J. Chem. Chem. Eng.* **2006**, *25*, 9−14.
(127) Musaddique, M.; Rafique, A.; Iqbal, J. Production of carbon nanotubes by different routes: A review. *J. Encapsulation Adsorpt. Sci.* **2011**, *1*, 29−34.
(128) Deshmukh, A. A.; Mhlanga, S. D.; Coville, N. J. Carbon spheres. *Mater. Sci. Eng., R* **2010**, *70*, 1−28.
(129) Cheng, L.; Liu, Y.; Zhang, J.; Yuan, D.; Xu, C.; Sun, G. Synthesis and application of spherical structured carbon materials. *Prog. Chem.* **2006**, *18*, 1298−1304.
(130) Jiménez, V.; Muñoz, A.; Sánchez, P.; Valverde, J. L.; Romero, A. Pilot plant scale synthesis of CNS: Influence of the operating conditions. *Ind. Eng. Chem. Res.* **2012**, *51*, 6745−6752.

(131) Pol, V. G.; Thiyagarajan, P.; Calderon Moreno, J. M.; Popa, M. Solvent-free fabrication of rare $LaCO_3OH$ luminescent superstructures. *Inorg. Chem.* **2009**, *48*, 6417−6424.
(132) Pol, V. G.; Calderon-Moreno, J. M.; Popa, M.; Acharya, S.; Ariga, K.; Thiyagarajan, P. Synthesis of new red-emitting single-phase europium oxycarbonate. *Inorg. Chem.* **2009**, *48*, 5569−5573.
(133) Lou, Z.; Chen, Q.; Zhang, Y.; Wang, W.; Qian, Y. Diamond formation by reduction of carbon dioxide at low temperatures. *J. Am. Chem. Soc.* **2003**, *125*, 9302−9303.
(134) Mosio-Mosiewski, J.; Warzala, M.; Morawski, I.; Dobrzanski, T. High-pressure catalytic and thermal cracking of polyethylene. *Fuel Process. Technol.* **2007**, *88*, 359−364.
(135) Chen, J. C.; W., Q.; Y., Y.; Q.. Low temperature synthesis and photoluminescence of cubic silicon carbide. *J. Phys. D: Appl. Phys.* **2006**, *39*, 1472.
(136) Wei, L.; Chen, Q.; Kong, X. Lithium storage properties of porous carbon formed through the reaction of supercritical carbon dioxide with alkali metals. *J. Am. Ceram. Soc.* **2011**, *94*, 3078−3083.
(137) Zhang, J.; Yan, B.; Zhang, F. Synthesis of carbon-coated Fe_3O_4 composites with pine-tree-leaf structures from catalytic pyrolysis of polyethylene. *CrystEngComm* **2012**, *14*, 3451−3455.
(138) Jianwei, L.; Wanjuan, L.; Xiangying, C.; Shuyan, Z.; Fanqing, L.; Yitai, Q. Fabrication of hollow carbon cones. *Carbon* **2004**, *42*, 669−671.
(139) Xiao, Y.; Liu, Y.; Mi, Y.; Yuan, D.; Zhang, J.; Cheng, L. A simple route to form straw-like carbon microbundles. *Chem. Lett.* **2005**, *34*, 1422−1423.
(140) Pol, V. G.; Pol, S. V; Gedanken, A. Core−shell nanorods of SnS−C and SnSe−C: Synthesis and characterization. *Langmuir* **2008**, *24*, 5135−5139.
(141) Lou, Z.; He, M.; Zhao, D.; Li, Z.; Shang, T. Synthesis of carbon nanorods by reduction of carbon bisulfide. *J. Alloys Compd.* **2010**, *507*, 38−41.
(142) Koprinarov, N.; Konstantinova, M. Exotic in shape particles obtained by low temperature pyrolysis of ferrocene. *Physica E* **2012**, *44*, 1054−1057.
(143) Pol, S. V; Pol, V. G.; Kessler, V. G.; Gedanken, A. Growth of carbon sausages filled with in situ formed tungsten oxide nanorods: Thermal dissociation of tungsten(VI) isopropoxide in isopropanol. *New J. Chem.* **2006**, *30*, 370−376.
(144) Chen, C.; Lou, Z. Formation of C_{60} by reduction of CO_2. *J. Supercrit. Fluids* **2009**, *50*, 42−45.
(145) Wang, Q.; Cao, F.; Chen, Q. Synthesis of hexagonal tungsten carbide in tungsten-sodium and supercritical carbon dioxide system. *Mater. Chem. Phys.* **2006**, *95*, 113−116.